ion and a spectrum was obtained by scanning the electric field of ESA-2 to obtain the product ion spectrum. Consecutive collisional activation experiments (MS/MS/MS) were conducted as previously described.[13]

The ZAB-T four-sector tandem mass spectrometer consisted of two high-mass, double-focusing mass spectrometers.[17] The design of MS-2 was a reverse geometry, Mattauch–Herzog type (BE). The instrument was equipped with a Cs ion gun and was capable of producing a 50-keV Cs$^+$ beam. For the negative ion SIMS experiment, the Cs gun was operated at ca. 17 kV so that the overall energy of the Cs$^+$ beam was approximately 25 keV. When full mass spectra were obtained, only MS-1 and the intermediate detector were used. When MS/MS experiments were conducted, MS-1 was used to select the precursor ion at a mass resolution of ca. 1500 and a B/E scan was taken with MS-2 to record the product ions produced by collisional activation in the collision cell located between MS-1 and MS-2. The object slit of MS-2 was closed so that the peak of the selected ion went from flat to round top (slit fully illuminated) so that the resolution of the product ions was ca. 1000 (FWHH).

Procedures. For acquiring a full scan mass spectrum, a few micrograms of the peptide was mixed with ca. 3 μL of the alkaline earth metal ion hydroxide-saturated glycerol/thioglycerol (1:1) on the tip of the FAB probe. The probe then was exposed to the 25-keV Cs$^+$ beam to cause desorption. In a typical experiment, the first ten 20-s scans following sample introduction were acquired and the signal averaged.

For FAB-MS/MS experiments, a few micrograms of the peptide was mixed on the tip of a FAB probe with the alkaline earth metal ion hydroxide or acetate in glycerol/thioglycerol (1:1). The tip was then exposed to a 25-keV Cs$^+$ ion beam on the ZAB-T instrument to cause desorption of the various metal-bound peptide ions.

For FAB-MS-MS-MS experiments,[13] the Kratos MS-50 was used. The source-produced ions were activated in the first field-free region, and the collision cell pressure was adjusted so that the product signal was maximized. The product ion of interest was selected by setting the first ESA and the magnet at appropriate values. This selected product ion was then collisionally activated in the third field-free region with 50% of main beam suppression, and the product ions were recorded by scanning the second ESA.

Acknowledgment. This work was supported by the U.S. National Science Foundation, Grant No. CHE9017250.

---

(17) Gross, M. L. Tandem Mass Spectrometry: Multisector Magnetic Instrument. In *Methods in Enzymology*; McCloskey, J. A., Vol. Ed.; Academic Press: San Diego, CA, 1990; Vol. 193, pp 131–153.

Molecular Complexes between Potassium and Ethylenediamine: Photoionization and ab Initio Molecular Orbital Studies

Y.-H. Liau[†] and T.-M. Su*[,†,‡]

Contribution from the Department of Chemistry, National Taiwan University, Taipei, Republic of China, and The Institute of the Atomic and Molecular Sciences, Academia Sinica, Taipei, Republic of China. *Received March 25, 1992*

Abstract: The molecular complexes formed between potassium and ethylenediamine (en), K(en) and K$_2$(en), were generated in a flow reactor and studied by photoionization mass spectrometry. The photoionization efficiencies of these complexes were analyzed with Watanabe plots, and the photoionization threshold energies were determined. Ab initio molecular orbital calculations were also performed for the neutral complexes and their corresponding positive ions. Supported by the calculation results, several conformers of K(en) in the photoionization efficiency spectrum were assigned. The photoionization threshold energies were measured to be 3.34, 3.54, and 3.64 ± 0.01 eV for three types of K(en) conformers and 3.57 ± 0.05 eV for the cyclic conformer of K$_2$(en), respectively. The upper bound of the enthalpy of the complex dissociation of K$_2$(en) into K$_2$ and ethylenediamine was determined to be 10.4 ± 1.5 kcal/mol. The conformational analysis of the potassium–ethylenediamine molecular complexes using photoionization spectrometry was reported for the first time. On the basis of the molecular orbital study, the structures and the nature of the bonding of these molecular complexes were also described.

1. Introduction

The molecular complexes formed between alkali metal atoms and Lewis base molecules have been under intensive investigation for the past decade or so.[1-16] Theoretical calculations were centered on the stabilities and the nature of these bonds.[1-11] To date, the gas-phase experiments have mainly concerned the measurement of the photoionization threshold energies and the photoionization efficiencies of these complexes.[12-16] A few of the experimental bond energies of the molecular complexes were deduced from these experiments.[12-14] Some high clusters containing sodium or cesium atoms were also reported.[12,13,15,16] Despite these theoretical and experimental efforts, the properties of the molecular complexes formed between alkali metal atoms and polyfunctional Lewis base molecules, such as the ethylenediamine molecule (en), were still not available. The interplay between the interactive forces of the complex bonding of alkali atom–ethylenediamine and the internal hydrogen bonding of the two amino groups of ethylenediamine had also not been touched.

In this article, we report the photoionization measurements and molecular orbital calculations on the molecular complexes formed

---

[†] National Taiwan University.

[‡] Academia Sinica.

(1) Nicely, V. A.; Dye, J. L. *J. Chem. Phys.* **1970**, *52*, 4795–4803.

(2) Trenary, M.; Schaefer, H. F., III; Kollman, P. A. *J. Am. Chem. Soc.* **1977**, *99*, 3885–3886.

(3) Trenary, M.; Schaefer, H. F., III; Kollman, P. A. *J. Chem. Phys.* **1978**, *68*, 4047–4050.

(4) Curtiss, L. A.; Frurip, D. J. *Chem. Phys. Lett.* **1980**, *75*, 69–74.

(5) Bentley, J.; Carmichael, I. *J. Phys. Chem.* **1981**, *85*, 3821–3826.

(6) Bentley, J. *J. Am. Chem. Soc.* **1982**, *104*, 2754–2759.

(7) Broughton, J. Q.; Bagus, P. S. *J. Chem. Phys.* **1982**, *77*, 3627–3634.

(8) Curtiss, L. A.; Pople, J. A. *J. Chem. Phys.* **1985**, *82*, 4230–4235.

(9) Curtiss, L. A.; Kraka, E.; Gauss, J.; Cremer, D. *J. Phys. Chem.* **1987**, *91*, 1080–1084.

(10) Wurthwein, E.-U.; Schleyer, P. v. R.; Pople, J. A. *J. Am. Chem. Soc.* **1984**, *106*, 6973–6978.

(11) Hsiao, Y.-W.; Chang, K.-M.; Su, T.-M. *Chem. Phys.* **1992**, *162*, 335–348.

(12) Schulz, C. P.; Haugstatter, R.; Tittes, H. U.; Hertel, I. V. *Phys. Rev. Lett.* **1986**, *57*, 1703–1706.

(13) Schulz, C. P.; Haugstatter, R.; Tittes, H. U.; Hertel, I. V. *Z. Phys. D: At., Mol. Clusters* **1988**, *10*, 279–290.

(14) Kuan, T.-C.; Jiang, R.-C.; Su, T.-M. *J. Chem. Phys.* **1990**, *92*, 2553–2558.

0002-7863/92/1514-9169$03.00/0

between the ethylenediamine molecule and the potassium atom and the potassium diatomic molecule, K(en) and K_2(en). The effects of the conformation of ethylenediamine on the photoionization efficiency spectra of the complexes were specifically investigated by molecular orbital calculations. The relation between the measured photoionization efficiency spectra and the conformations of the neutral ground state and its corresponding cationic state was also established. Ethylenediamine is one of the simplest polyfunctional compounds. The present study should give us a better understanding of one general class of the chemistry of molecular complexes, the host–guest chemistry.[17]

2. Experimental Section

The generation and the photoionization measurements of the molecular complexes were carried out by a photoionization mass spectrometer coupled with a flow reactor. The general experimental setup has been given in previous publications.[14,18] Some refinements were made in the present experiment. The experimental conditions and the modifications are briefly described in the following paragraphs.

Potassium vapor was generated in a 493 K potassium oven and then was injected into the flow reactor with the help of an Ar flow. Liquid ethylenediamine was heated to a temperature of about 340 K, and the vapor was also injected into the reactor. The partial pressure of the ethylenediamine vapor in the main flow was kept at around 40 mTorr. A third flow of pure Ar, which served as a buffer gas for the flow system, was also introduced into the reactor. The potassium vapor, the ethylenediamine vapor, and the main argon buffer gas were all mixed well in the main flow reactor. The flow reactor was thermally regulated and the temperature was monitored by thermocouples. The total gas pressure of the final flow was kept at around 2.5 Torr during experiments. The composition of the flow reactor was then sampled by a 1-mm orifice and then collimated by a skimmer. The vacuum chambers were differentially pumped.

The molecular beam, being essentially a thermal beam, was photoionized at right angles either by conventional UV–vis radiation of a Hg lamp or by a tunable pulsed-laser beam. The laser system consisted of an excimer pumped dye laser and a second harmonic generator with a maximum wavelength line width of 0.003 nm. In the experiment the laser energy was continuously monitored by a pyroelectric joulemeter. All of the photoionization efficiency spectra were normalized to the laser photon number. Since the output of dye laser varied significantly over the tuning range of each dye and, in the present experiments, we usually needed several dyes to cover the wavelengths we were interested in, the photoionization efficiency spectra usually show a variation of the signal-to-noise ratio over the whole spectral range. The spectral response of the joulemeter over the present wavelength region is essentially flat. The ions formed by photoionization of the complexes in the interaction zone were mass selected by a quadrupole mass analyzer and detected by a channeltron electron multiplier. The control of the experiment and the analysis of the experimental data were all done by a microcomputer.

3. Ab Initio Molecular Orbital Calculations of K(en) and K_2(en) and Their Cations

All of the ab initio molecular orbital calculations were performed with either restricted or unrestricted Hartree–Fock theory (HF) using the Gaussian 90 package of computer codes.[19] Electron correlation was calculated by Moller–Plesset perturbation theory up to the second order (MP2).

The following optimization procedure of the complex geometry was done at the HF level. The standard 6-31g basis sets were used for the hydrogen atom and the second row elements. The potassium basis set was adapted from the Wachters' contracted [8s,4p] set of the (14s,9p) basis set.[20] For the calculations of the bond dissociation energies and ionization potentials, which include the MP2 calculations, 6-31g* basis sets were used for the C, N, and H atoms. The Wachters' basis set of K was augmented by the (2d) polarization functions of Klein et al.[21]

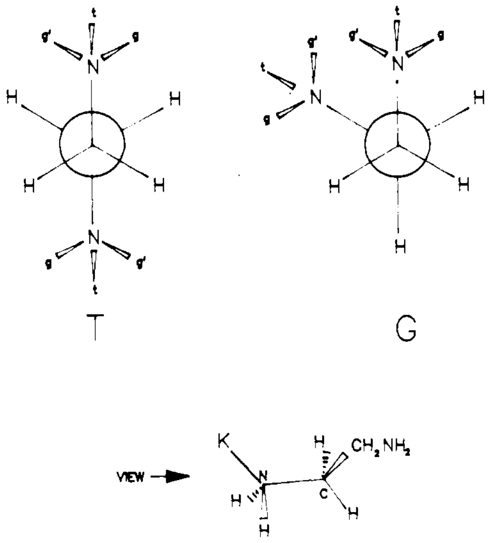

Figure 1. Conformation assignments of K(ethylenediamine).

In the calculation of the bond dissociation energies, the basis set superposition error (BSSE) was evaluated by the counterpoise method. The counterpoise correction is equal to the difference in energy between the isolated subunits on one hand and the subunit energies, each calculated within the basis set and geometry of the entire complex, on the other. The interaction energies calculated with the above procedures were interpreted as sudden dissociation energies. Since the BSSE was negligible for the conformation transformation of ethylenediamine itself, the adiabatic dissociation energy was defined as the sum of the sudden dissociation energy and the energy released in the geometry relaxation process of the subunits. All of the tabulated bond dissociation energies were corrected with these procedures.

Ethylenediamine has 10 possible conformers.[22-24] Since the complex bonding between the potassium atom and the amino group lies along the general direction of the tetrahedral lone pair electrons of the nitrogen atom, the notation here for the conformations of K(en) and K_2(en) follows the convention of the ethylenediamine molecule and is shown in Figure 1. The relative orientations of the C–C and the two C–N bonds are defined by the dihedral angles of KNCC, NCCN, and CCN:. Here the symbol of the colon represents the direction of the tetrahedral lone pair electrons of the nitrogen atoms. According to convention, the symbols t, g', and g indicated in Figure 1 refer to the appropriate trans (180°), gauche (60°), and anti-gauche (−60°) orientations, respectively. In this report, instead of the above strict orientations, these symbols are used in a more loose sense and should only be regarded as a general conformation notation.

For the ethylenediamine molecule, ab initio geometry optimization at the HF/4-21g level has been carried out by van Alsenoy et al.,[24] and the geometries of the 10 conformers were characterized. In this report, all of the energy calculations at higher levels were based on these geometric parameters and were designated as HF/6-31g*//4-21g and MP2/6-31g*//4-21g. As for the calculations of K(en) and K_2(en), because of the relatively weak bonding nature of the molecular complexes, the introduction of the potassium atoms only induces minor changes in the primary geometry of the Lewis bases. The major effect of the complex formation on the geometric parameters is related to the conformations of these complexes. The following calculations proceeded with this observation in mind.

---

(15) Hertel, I. V.; Huglin, C.; Nitsch, C.; Schulz, C. P. *Phys. Rev. Lett.* **1991**, *67*, 1767–1770.

(16) Misaizu, F.; Tsukamoto, K.; Sanekata, M.; Fuke, K. *Chem. Phys. Lett.* **1992**, *188*, 241–246.

(17) Vogtle, F.; Weber, E. *Host Guest Complex Chemistry/Macrocycles*; Springer-Verlag: Berlin, 1985.

(18) Jiang, R.-C.; Su, T.-M. *Chem. Phys. Lett.* **1991**, *181*, 373–377.

(19) Frisch, M. J.; Head-Gordon, M.; Trucks, G. W.; Foresman, J. B.; Schlegel, H. B.; Raghavachari, K.; Robb, M. A.; Binkley, J. S.; Gonzalez, C.; Defrees, D. J.; Fox, D. J.; Whiteside, R. A.; Seeger, R.; Melius, C. F.; Baker, J.; Martin, R. L.; Kahn, L. R.; Stewart, J. J. P.; Topiol, S.; Pople, J. A. *Gaussian 90*; Gaussian Inc.: Pittsburgh, PA, 1990.

(20) Wachters, A. J. H. *J. Chem. Phys.* **1970**, *52*, 1033–1036.

(21) Klein, M. L.; Goddard, J. D.; Bounds, D. G. *J. Chem. Phys.* **1981**, *75*, 3909–3915.

(22) Radom, L.; Lathan, W. A.; Hehre, W. J.; Pople, J. A. *J. Am. Chem. Soc.* **1973**, *95*, 693–698.

(23) Rasmussen, K.; Tosi, C. *Acta Chem. Scand. A* **1983**, *37*, 79–91.

(24) Van Alsenoy, C.; Siam, K.; Ewbank, J. D.; Schafer, L. *J. Mol. Struct. (Theochem)* **1986**, *136*, 77–91.

Table I. Theoretical Molecular Parameters and Mulliken Population Analysis[a]

species	r(KN)	∠KNC	∠KNCC	r(KK)	∠KKN	∠KKNC	charge of K[b]
K_2				4.170			0
K(MA)[c]	2.890	114.6					−0.038
K(g′Gg′)	2.833	115.4	41.8				−0.065
K(tGg′)	2.868	116.6	167.0				−0.043
K(gGg′)	2.877	120.0	282.7				−0.046
K(tTt)	2.905	114.5	180.0				−0.039
K_2(g′Gg′)	2.834	115.3	41.6	4.360	151.2	166.5	0.181,[e] −0.239[f]
K_2(tGg′)	2.848	114.2	166.8	4.276	171.8	81.9	0.142,[e] −0.187[f]
K_2(gGg′)	2.856	117.0	284.5	4.270	173.9	289.5	0.143,[e] −0.192[f]
K_2(tTt)	2.884	111.9	180.0	4.253	176.6	180.0	0.096,[e] −0.140[f]
K^+(MA)[c]	2.787	111.0					0.965
K^+(g′Gg′)	2.776	114.9	38.6				0.946
K^+(tGg′)	2.761	112.6	160.2				0.960
K^+(gGg′)	*d*						
K^+(tTt)	2.803	108.6	180.0				0.962
K_2^+(g′Gg′)	2.781	114.7	41.4	5.062	148.6	167.4	0.686,[e] 0.253[f]
K_2^+(tGg′)	2.777	112.9	164.9	4.897	172.8	170.1	0.647,[e] 0.305[f]
K_2^+(gGg′)	2.779	115.2	287.9	4.904	173.3	210.3	0.641,[e] 0.308[f]
K_2^+(tTt)	2.812	108.9	180.0	4.860	175.5	180.0	0.615,[e] 0.338[f]

[a] Distances in Å, angles in degrees, and electric charges in elementary charge. [b] 6-31g*. [c] MA is methylamine. [d] Local energy minimum is not found at the K^+(gGg′) conformation. [e] The potassium atom which is close to the nitrogen atom of ethylenediamine. [f] The potassium atom which is away from the nitrogen atom of ethylenediamine.

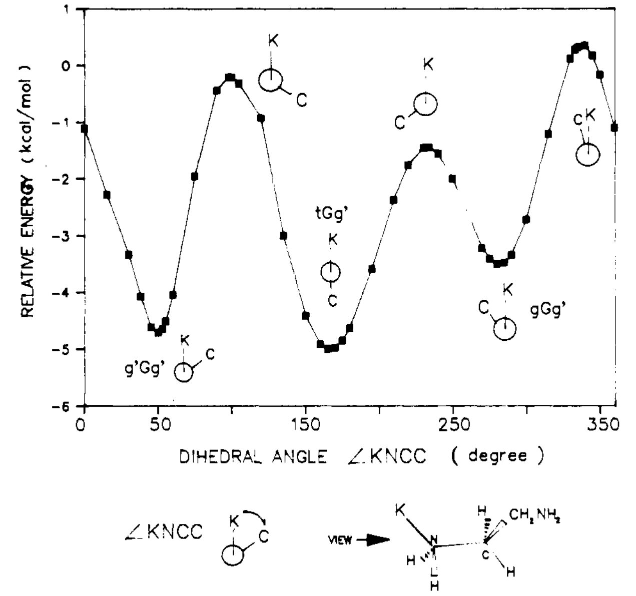

Figure 2. Relative potential energy of K(en) as a function of the dihedral angle KNCC. The square points (■) represent the calculated data, and the smooth curve is the linear connection between the data points. The zero potential is set at the dissociated states of K and the conformer of ethylenediamine tGg′.

To begin with, the internal rotation of the NH_2K group along the NC bond was considered first. The most stable conformer of ethylenediamine at the HF/6-31g* level was determined to be tGg′. The potassium atom was then brought in, and the position was optimized with the structure of en(tGg′) being fixed at the equilibrium geometry. The geometry of the complex K(tGg′) was then frozen, and the one-dimensional potential energy with the internal rotation of the NH_2K group along the NC bond was calculated with the 6-31g basis. The result is shown in Figure 2. The three local minima are identified as K(g′Gg′), K(tGg′) and K(gGg′), respectively, in which K(g′Gg′) has a cyclic structure while K(tGg′) and K(gGg′) are noncyclic with an internal hydrogen bond.

A full calculation of all of the conformations of K(en) and K_2(en) is computationally intensive. Nevertheless, for the elucidation of the present photoionization data, which reflect energetically the stable neutral states and the vertical ionic states of these complexes simultaneously, one only needs to consider three categories of conformations: the cyclic form, the noncyclic forms with internal hydrogen bonding, and the noncyclic forms without hydrogen bonding. For the present consideration, in addition to the above three stable conformations mentioned previously, the noncyclic conformer without hydrogen bonding K(tTt) was added as a representative of the type three conformers, such as K(tTg), K(gGg), etc. All of these type three conformers of ethylenediamine have similar potential energies.[22-24] The complexation energies of these conformers with the potassium atom are expected to be similar too.

The final conformation structures of the K(en) complex were determined by optimizing the dihedral angles of both amino groups and the position of the potassium atom with respect to the lone pair electrons of the amino group at HF/6-31g. In a similar way, the optimized conformations of K_2(en) were obtained. Single-point MP2/6-31g* calculations were then performed on all of the partially optimized geometries. The corresponding positive ions were also calculated in the same manner. The above optimization procedure was checked by calculating the equilibrium bond dissociation energies of $K(CH_3NH_2)$ and $K^+(CH_3NH_2)$, which yielded 4.3 and 19.3 kcal/mol for these two complexes, respectively. Compared with the values of 3.6 and 18.3 kcal/mol which resulted if the complete complexes were geometrically optimized at HF/6-31g and then energetically calculated at MP2/6-31g* with BSSE correction, the systematic deviation between these two procedures was estimated to be 0.7 kcal/mol for the neutral species and 1.0 kcal/mol for the ionic species considered in this study.

4. Results and Discussion

4.1. Structures and Bonding of K(en), K_2(en), K^+(en), and K_2^+(en). Theoretical Results. The geometry indexes, the Mulliken population of potassium, the dissociation energies, and the ionization energies of these complexes were calculated and are listed in Tables I–III.

4.1.1. K(en) and K^+(en). Figure 3 shows the ball-and-stick representations of the four conformers of K(en). K(g′Gg′) is a cyclic form, K(gGg′) and K(tGg′) are conformers with internal hydrogen bonding, and K(tTt) is a straight-chain complex. As a reference, the complex formed between the potassium atom and methylamine, $K(CH_3NH_2)$, was also studied and is listed in the tables.

As shown in Table I, the bond lengths of KN among these molecular conformers are close to each other, with an average value of about 2.87 Å. However, a closer comparison reveals that the bond lengths of K(tTt) and $K(CH_3NH_2)$ are a little longer than those of the others. Overall, the cyclic form K(g′Gg′) has the shortest KN bond length. The charge population of the potassium atom, an indication of the extent of charge transfer in the formation of the complex, also reflects a similar trend. The potassium atom of the cyclic form K(g′Gg′) has almost twice as much negative charge as the potassium in the other conformers.

Table II. Theoretical Equilibrium Dissociation Energies (kcal/mol)

	sudden		adiabatic			
reactions	HF	MP2	HF[a]	MP2[a]	HF[b]	MP2[b]
$K(MA)^c \rightarrow K + MA$	3.4	4.4	2.8	3.6		
$K(g'Gg') \rightarrow K + en$	9.6	11.3	4.1	4.8	8.5	9.9
$K(tGg') \rightarrow K + en$	4.1	5.0	3.8	4.8	3.8	4.8
$K(gGg') \rightarrow K + en$	3.6	4.7	2.3	2.9	2.5	3.1
$K(tTt) \rightarrow K + en$	3.2	4.2	1.5	1.9	3.2	3.9
$K_2(g'Gg') \rightarrow K_2 + en$	14.1	14.4	8.4	7.4	12.8	12.4
$K_2(tGg') \rightarrow K_2 + en$	6.9	7.1	6.6	6.7	6.6	6.7
$K_2(gGg') \rightarrow K_2 + en$	6.6	7.0	5.3	5.0	5.4	5.2
$K_2(tTt) \rightarrow K_2 + en$	5.5	5.9	3.8	3.4	5.5	5.4
$K^+(MA)^c \rightarrow K^+ + MA$			19.1	18.3		
$K^+(g'Gg') \rightarrow K^+ + en$			31.0	30.9	35.5	35.9
$K^+(tGg') \rightarrow K^+ + en$			23.1	24.1	23.1	24.1
$K^+(gGg') \rightarrow K^+ + en$			*d*			
$K^+(tTt) \rightarrow K^+ + en$			16.5	16.8	18.2	18.8
$K_2^+(g'Gg') \rightarrow K_2^+ + en$			22.3	22.3	26.8	27.3
$K_2^+(tGg') \rightarrow K_2^+ + en$			16.8	17.5	16.8	17.5
$K_2^+(gGg') \rightarrow K_2^+ + en$			16.2	15.7	16.4	15.9
$K_2^+(tTt) \rightarrow K_2^+ + en$			11.5	11.7	13.2	13.8
$K_2^+(g'Gg') \rightarrow K + K^+(g'Gg')$			3.0	3.5		
$K_2^+(tGg') \rightarrow K + K^+(g'Gg')$			−3.6	−4.0		
$K_2^+(gGg') \rightarrow K + K^+(g'Gg')$			−5.0	−5.5		
$K_2^+(tTt) \rightarrow K + K^+(g'Gg')$			−8.9	−10.0		

[a] Adiabatic equilibrium dissociation energy with respect to the most stable conformer of ethylenediamine, tGg′. [b] Adiabatic equilibrium dissociation energy with respect to its own conformer state. [c] MA is methylamine. [d] Local energy minimum is not found at the K⁺(gGg′) conformation.

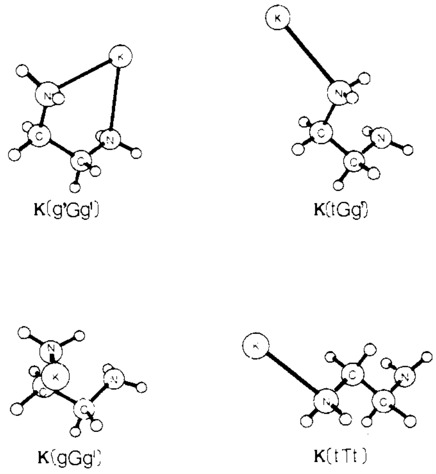

Figure 3. Geometric structures of four K(en) conformers: K(g′Gg′), K(tGg′), K(gGg′), and K(tTt).

Overall, the potassium atom in the monodentate form without hydrogen bonding, i.e., K(tTt), contains the least charge.

The corresponding K⁺(en) has different stable conformations. The cyclic form is still the most stable conformer, while one of the two conformers with internal hydrogen bonding, K⁺(gGg′), is not stable and would decay classically to the cyclic form. In other words, there is no potential barrier between K⁺(gGg′) and K⁺(g′Gg′) at the present level of calculation. The other two conformers, K⁺(tGg′) and K⁺(tTt), remain locally stable with respect to their conformations. The bond distances between K⁺ and N are consistently shorter than those of the neutral conformers.

Table II lists two types of equilibrium dissociation energies used in this study: the sudden dissociation energy and the adiabatic equilibrium dissociation energy. The sudden dissociation energy of a conformer is defined as the dissociation energy relative to the free potassium atom and the ethylenediamine whose geometry is frozen in the form of the parent complex. The adiabatic equilibrium dissociation energy can be further divided into two types, which are defined as the dissociation energy relative either to the free potassium atom and the most stable conformation of ethylenediamine, tGg′, or to the free potassium atom and its own locally stable conformer of ethylenediamine. Both types of adiabatic dissociation energies are listed in Table II. The sudden dissociation energy serves as a measure for the direct interaction strength between the potassium atom and the conformers of ethylenediamine. The adiabatic equilibrium dissociation energy serves as a measure for the thermodynamic dissociation energy.

As shown in Table II, the sudden dissociation energy of the cyclic conformer, K(g′Gg′), is approximately twice as large as that of the other three conformers. The sudden dissociation energies of the two conformers with internal hydrogen bonding are approximately equal to each other and in turn are only slightly larger than that of the straight-chain conformer, K(tTt). These data suggest that the direct interaction strength involved in complexation between the potassium atom and the amino group of ethylenediamine is additive. The extents of the charge transfer in the Mulliken population analysis also support this statement. The adiabatic dissociation energy with respect to the most stable conformer tGg′ indicates that the adiabatic dissociation energy of the cyclic form K(g′Gg′) is close to that of K(tGg′), a conformer with internal hydrogen bonding. These two conformers constitute the most stable forms of the conformation. As expected, the other two conformers are less stable, and K(tTt) has the highest potential energy. The findings suggest that, in a gas-phase thermodynamic system, the cyclic conformer and the conformers with internal hydrogen bonding will dominate over the other conformations. The adiabatic dissociation energy of the complex with respect to its parent conformation serves as a measure of the energy difference between the stable potassium complex and its dissociated local minimum. As shown in Table II, these values are close to their sudden dissociation energies. This suggests that the complexation of the potassium atom does not perturb the conformations of the parent ethylenediamine molecule much.

The relative stabilities of these conformers come from the extent of complexation of the potassium atom with the two amino groups and the strength of the internal hydrogen bonding. For the cyclic form, the simultaneous complexation of the potassium atom with both amino groups outweighs the anti-hydrogen bond configuration of the amino groups. The simultaneous existence of one potassium complexation bond and one hydrogen bond also stabilizes the complex system.

The corresponding ionic states also show a similar trend in the dissociation energies. The only major difference is that the ion–electric dipole interaction is so much stronger than the complexation energy of a potassium atom with an amino group that the interaction of the internal hydrogen bonding becomes less important in the determination of the dissociation energy. This very reason could also be used to explain the absence of a local minimum for the K⁺(gGg′) conformer.

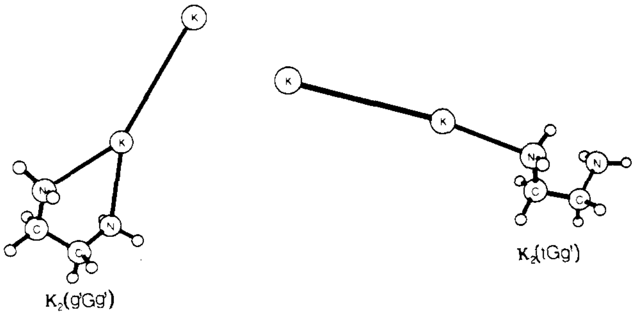

Figure 4. Geometric structures of the $K_2(en)$ conformers $K_2(g'Gg')$ and $K_2(tGg')$.

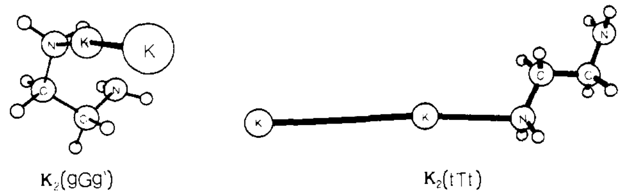

Figure 5. Geometric structures of the $K_2(en)$ conformers $K_2(gGg')$ and $K_2(tTt)$.

4.1.2. $K_2(en)$ and $K_2^+(en)$. The four conformers of $K_2(en)$ are shown in Figures 4 and 5. The geometry indexes and Mulliken populations of the potassium atoms are shown in Table I. For $K_2(en)$ the bond lengths between the potassium atom directly bonded to the amino group and the ethylenediamine are close to those of K(en). The major change comes from the second potassium atom. Compared with the internuclear distance of K_2, the bond length of K_2 in $K_2(en)$ is longer by as much as 0.19 Å in the cyclic conformation. The straight-chain conformer shows the least lengthening at 0.08 Å. The net charge transfer from ethylenediamine to K_2 is almost the same as that for the corresponding K(en) conformers. However, the charge separation between the potassium atoms is as large as 0.181 e for the cyclic form. The straight-chain conformer also has a charge separation of 0.096 e, almost half the value of the cyclic form. The two conformers with internal hydrogen bonding have a charge separation in between these two values. Table II shows the sudden dissociation energies and the adiabatic equilibrium dissociation energies of $K_2(en)$. In comparing the sudden dissociation energies of $K_2(en)$ with those of K(en), one finds that, for each complexation bonding, $K_2(en)$ is more stable than K(en) by an average of 2.3 kcal/mol at the MP2 level. The adiabatic equilibrium dissociation energies of the conformers of $K_2(en)$ are also consistently much higher than those of K(en). The cyclic form has the highest stability, and the straight-chain conformer is the least stable one.

For the ionic states, the bonding distances between N and K are consistently shorter than those of the corresponding neutral states. However, the KK distances are longer than those of the neutral states by an average of 0.64 Å. In contrast to the $K^+(en)$ ion, all four conformations of $K_2^+(en)$ are locally stable. Otherwise, the general pattern of the adiabatic dissociation energies is similar to the $K^+(en)$ case.

4.1.3. Nature of the Bonding of K(en) and $K_2(en)$. For the potassium–Lewis base complexes, it has been recognized that electron correlation effects, electrostatic interactions, and dipole–induced dipole interactions all take part in the stabilization of the complexes.[11] In comparing the sudden dissociation energies of $K(CH_3NH_2)$, K(en), and $K_2(en)$, one finds that at the MP2 level the interaction strengths of the bidentates are about twice those of the monodentates. Among the sudden dissociation energies, the electron correlation effect contributes more stabilization energy for the monopotassium systems than for the dipotassium systems. At the MP2 level, the electron correlation factor does not affect the stability of the $K_2(en)$ complexes much. In comparing the mono- and dipotassium systems, one finds that the interaction strengths of $K_2(en)$ are consistently stronger than those of K(en) by about 2.3 kcal/mol for each K–N complex bond. From the Mulliken population analysis of the potassium atoms, the extent of charge transfer from ethylenediamine to potassium atoms is similar between these two mono- and dipotassium complexes. However, as mentioned previously, the charge polarization of K_2 in $K_2(en)$ is quite significant. The electric polarizabilities of K and K_2 are 43.4 and 61 Å^3, respectivley. Although it is difficult to quantify this factor in terms of the stabilization energy, nevertheless, the comparatively large electric polarizability of K_2 suggests that the extra stability of $K_2(en)$ could be attributed mainly to the charge polarization effect.

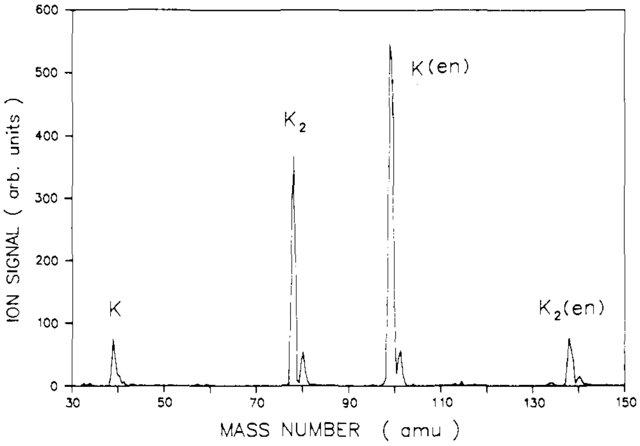

Figure 6. Photoionization mass spectrum of K(en) and $K_2(en)$ under the broadband UV radiation of a Hg lamp.

The final stabilization of the potassium complexes, to the first-order approximation, depends on the adiabatic relaxation energy between the suddenly dissociated ethylenediamine and its equilibrium conformer. The energy change of this process is dominated by the hydrogen bonding between the two amino groups. For this reason, although the cyclic conformers possess the highest sudden dissociation energies (the direct complexation energies), and because of the anti-hydrogen-bonding orientation of the two amino groups, the final stabilization energies are reduced by about 7 kcal/mol for both the mono- and dipotassium systems. On the other hand, the conformers with internal hydrogen bonding have the extra stability caused by the presence of hydrogen bonding. Finally, as expected, the straight-chain complex without hydrogen bonding has the lowest stability.

4.2. Photoionization Mass Spectra of K(en) and $K_2(en)$. Figure 6 shows the photoionization mass spectrum of the potassium flow system in the presence of 40 mTorr of ethylenediamine vapor at broadband UV radiation. Under a pure potassium flow, the only detected photoionization mass peaks were K^+ (39,41) and K_2^+ (78,80). After the introduction of the ethylenediamine vapor, the major peaks were K^+, K_2^+, $K^+(en)$ (99,101), and $K_2^+(en)$ (138,140). Upon turning off the ethylenediamine flow, all signals of the potassium complexes disappeared. This suggested that $K^+(en)$ and $K_2^+(en)$ originated from the direct gas-phase recombination reaction between en and potassium atoms or molecules. All of the mass peaks disappeared immediately if one turned off the potassium flow. It should be noted that no hypermetallic compounds of ethylenediamine were found in the mass spectrum. This is in contrast with our previous finding regarding the reactions between potassium and other Lewis bases such as H_2O and NH_3, in which hypermetalated compounds such as K_2OH and K_2NH_2 were generated.[14,18]

The relative ion signals of K_2 and $K_2(en)$ varied as the temperature of the flow reactor changed. Considering the temperature of the sampling orifice to be the final local quasiequilibrium temperature of the flow reactor, the equilibrium constant K_e of the complexation reaction $K_2(g) + en(g) \rightleftarrows K_2(en)(g)$ may be expressed as

$$K_e = \frac{P(K_2(en))}{P(K_2)P(en)} \tag{1}$$

in which P is the partial pressure of each component. In the photoionization experiments, one would measure the ion signals of $K_2(en)$ and K_2. The equilibrium constant of the ion signal, K_e^i, is defined as

$$K_e^i = \frac{I(K_2^+(en))}{I(K_2^+)P(en)} \tag{2}$$

If the photoionization energy is higher than the ionization threshold energies of K_2 and $K_2(en)$ and if during photoionization $K_2(en)$ does not dissociate into K_2^+ and ethylenediamine, conditions that usually can be met because, for this type of complexes, the interaction strength of the ionic species is consistently stronger than those of the neutral species globally,[25] then the ion signals can be directly related to their neutral parent molecules by the relation[25,26]

$$I(K_2^+(en)) = \epsilon(K_2(en))\mu(K_2(en))\sum_i\sum_f F_{fi}B_i(K_2(en)) \tag{3}$$

in which $\epsilon(K_2(en))$ represents the detection efficiency of the experimental apparatus for the $K_2^+(en)$ ion and other photoionization-related constants, $\mu(K_2(en))$ is the electronic oscillation strength from the ground to the ionic state, F_{fi} is the Franck–Condon factor from the initial bound vibrational state i to the final bound vibrational state f of the ion, and $B_i(K_2(en))$ is the Boltzmann factor of the ith vibrational state. A similar expression could be written for K_2. In writing down the above expressions, we have tacitly assumed the Born–Oppenheimer approximation and also the weak dependency of the electronic transition strength on the vibration states.

In general, $\sum_f F_{fi}B_i \le B_i$, with the equality holding if the initial vibrational wave function can be confined by the final ionic potential. Under this confinement condition, the equilibrium constant K_e is proportional to the equilibrium constant of the ion signals, K_e^i. The van't Hoff plot of K_e^i should yield the enthalpy of the reaction. For the other situation in which part of the photoionization products ended up in other ionic fragments, the K_e^i would be a measure of the equilibrium constant of the neutral species with their concentrations being weighted by the Franck–Condon factors of the bound states. In other words, the Franck–Condon factors between bound vibrational states could be regarded as a sampler for a certain energy region of the neutral species. In this sense the van't Hoff plot of K_e^i would reflect the thermodynamic energy relation between the sampled energy states of the neutral species involved.

For K_2 and K_2^+, because K_2^+ has a deeper potential than that of K_2[27,28] and because at room temperature 99% of the K_2 population is still confined by the K_2^+ ionic potential, the ion signal $I(K_2^+)$ is directly proportional to $P(K_2)$. For $K_2(en)$ and $K_2^+(en)$, as shown in Table II, only $K_2^+(g'Gg')$ will survive energetically. The other conformers will eventually dissociate into K and $K^+(en)$. Note that, for this dissociation channel, the adiabatic dissociation energies of the conformers of $K_2^+(en)$ are within 0.5 kcal/mol of the sudden dissociation energies if the ionic geometries are frozen at the equilibrium geometries of the neutral species. The ion signal $I(K_2^+(en))$ is therefore sampling the neutral species around its lower vibrational states. The van't Hoff plot of eq 2 then yields an upper bound of the enthalpy of the complex dissociation.

Figure 7 shows the van't Hoff plot of the photoionization signal ratio of these two species. From the slope of the plot, the upper bound of the enthalpy of complexation is determined to be 10.4 ± 1.5 kcal/mol. The 1.5 kcal/mol error is mainly due to the estimated uncertainty in the flow temperature. Because of the undetermined proportionality constant between K_e and K_e^i, the entropy of complexation was not obtained in this study.

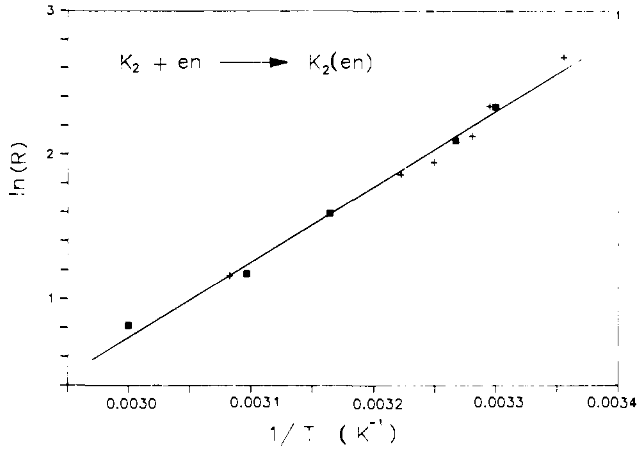

Figure 7. van't Hoff plot of the photoionization signal ratio of the reaction K_2 + en → $K_2(en)$. The square (■) and cross (+) data points indicate two independent measurements.

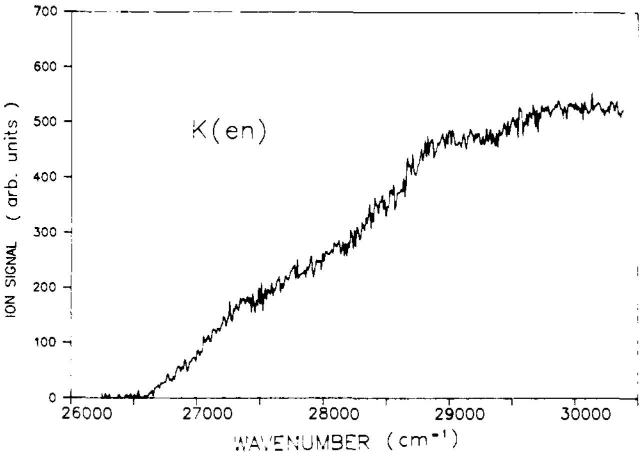

Figure 8. Photon-number-normalized photoionization efficiency spectrum of K(en) at 303 K.

4.3. Photoionization Efficiency Measurements of K(en) and K_2(en). Figures 8–10 show the photoionization efficiency spectra of K(en) and $K_2(en)$. In interpreting these spectra one usually needs to consider the following factors related to the photoionization process: (a) the presence of isomers; (b) the thermal population of neutral species; (c) the Franck–Condon factors; (d) the electronic transition strength between the neutral and the ionic states; (e) other competing processes; and (f) the ions that are produced from different parent neutral species. Frequently it is difficult to justify whether a certain contributing factor is more important than the others. This leads to uncertainties in determining the precise ionization potential. In the following discussion, the results of the molecular orbital calculations were employed to interpret these photoionization efficiency spectra. Since the thermal equilibrium condition is assumed in the flow system and the bonding in these molecular complexes is weak, the Watanabe method for the treatment of photoionization efficiency spectra is adapted in the present study.[29]

4.3.1. K(en). Figure 8 shows the photoionization efficiency spectrum of K(en). The plot of the logarithm of the ion signals vs photon energy (Watanabe plot) is also given in Figure 9. The straight lines are the result of least-squares fitting. To ensure that the spectrum was not contaminated by the possible photofragments of $K_2(en)$, the spectrum was checked by the reduction of the concentration of K_2 and then $K_2(en)$ through the increase of the

---

(25) Su, T.-M. *Chem. Phys.* **1990**, *144*, 93–101.

(26) Siegbahn, H.; Karlsson, L. In *Handbuch Der Physik/Encyclopedia of Physics*; Mehlhorn, W., Ed.; Springer-Verlag: Berlin, 1982; Vol. 31, pp 294–296.

(27) Tango, W. J.; Link, J. K.; Zare, R. N. *J. Chem. Phys.* **1968**, *49*, 4264–4268.

(28) Broyer, M.; Chevaleyre, J.; Delacretaz, G.; Fayet, P.; Woste, L. *Chem. Phys. Lett.* **1985**, *114*, 477–482.

(29) Kappes, M. M.; Schar, M.; Rothlisberger, U.; Yeretzian, C.; Schumacher, E. *Chem. Phys. Lett.* **1988**, *143*, 251–258.

(30) Moore, C. E. *Atomic Energy Levels*; US GPO: Washington, DC, 1971; Vol. 1, NSRD-NBS, pp 227–229.

(31) Broyer, M.; Chevaleyre, J.; Delacretaz, G.; Martin, S.; Woste, L. *Chem. Phys. Lett.* **1983**, *99*, 206–212.

Table III. Theoretical and Experimental Ionization Potentials (eV)

	vertical		adiabatic				
reaction	HF	MP2	HF[a]	MP2[a]	HF[b]	MP2[b]	exptl
$K \rightarrow K^+$			4.00	4.04			4.339[e]
$K_2 \rightarrow K_2^+$	3.44	3.69	3.39	3.67			4.064[f]
K(MA)[c] → K^+(MA)	3.35	3.42	3.29	3.34			
K(g′Gg′) → K^+(en)	2.89	3.00	2.85	2.95	2.85	2.95	3.34[g]
K(tGg′) → K^+(en)	3.20	3.27	2.82	2.85	3.16	3.21	3.54[g]
K(gGg′) → K^+(en)	3.20	3.27	2.75	2.78	*d*		3.54[g]
K(tTt) → K^+(en)	3.36	3.43	2.71	2.72	3.35	3.41	3.64[g]
K_2(g′Gg′) → K_2^+(en)	2.75	3.01	2.72	3.01	2.72	3.01	3.57[g]
K_2(tGg′) → K_2^+(en)	2.94	3.19	2.62	2.87	2.90	3.18	
K_2(gGg′) → K_2^+(en)	2.95	3.20	2.56	2.81	2.90	3.18	
K_2(tTt) → K_2^+(en)	3.06	3.31	2.49	2.72	3.01	3.29	

[a] Adiabatic ionization potential with respect to the most stable conformer K^+(g′Gg′) or K_2^+(g′Gg′). [b] Adiabatic ionization potential with respect to its own conformer state. [c] MA is methylamine. [d] Local energy minimum is not found at the K^+(gGg′) conformation. [e] From ref 30. [f] From ref 31. [g] This work.

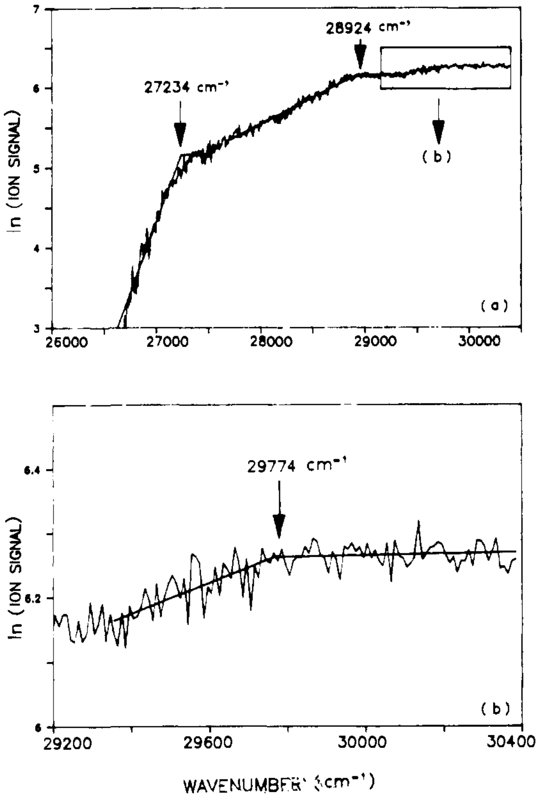

Figure 9. Watanabe plot of the photoionization efficiency spectrum of K(en).

flow tube temperature. The features of the spectrum remained unchanged. This may be attributed to the relatively minor concentration of K_2(en) and/or the inefficient collection efficiency of the ion lenses for the fragment ions with extra translational energy. This extra translational energy is spatially isotropic.

As shown in Figures 8 and 9, three distinct steps are found and the points of break can be determined to be 3.34, 3.54, and 3.64 ± 0.01 eV, respectively. The uncertainty was estimated by taking the uncertainty of the linear fit of the lowest ionization threshold energy, which happened to have the largest fitting uncertainty of these three threshold energies. This value is on the order of one-half of the thermal energy at 300 K. On the theoretical side, as shown in Table III, vertical ionization potentials were predicted to be 3.00, 3.27, 3.27, and 3.43 eV for the K(g′Gg′), K(tGg′), K(gGg′), and K(tTt) conformers, respectively, at the MP2 level. With the acknowledgement that MO calculations using the Gaussian 90 package usually predict a consistently lower ionization potential, the general offset between the experimental and theoretical values is not too surprising.[10,11] If one takes the different between the theoretical and experimental ionization potentials of the free potassium atom, 0.30 eV, to offset the theoretical vertical ionization potentials of K(en) conformers, one would find that the agreement is within 0.04 eV for each conformer, except K(tTt) for which the deviation is 0.09 eV. Note that we have adopted the straight chain conformer, K(tTt), as a representative of the general noncyclic conformers without internal hydrogen bonding. A slightly higher theoretical photoionization potential is expected. One could go further and compare the ionization potential differences between these conformers. Starting from the lowest ionization energy species, the experimental results show that the differences between the three distinguishable ionization thresholds are 4.7 and 2.3 kcal/mol. Molecular orbital calculations predict differences of 6.0 and 3.7 kcal/mol, respectively. Comparison of the above theoretical and experimental results, and given the approximation in considering the type three conformers, reveals that the agreement is good. The three points of break observed in the Watanabe plot could be reasonably assigned as the onsets of the photoionization of the three different types of structures classified in the previous theoretical section. These are the cyclic form, the noncyclic form with internal hydrogen bonding, and the noncyclic form without internal hydrogen bonding.

Overall, the photoionization efficiency spectrum of K(en) could be explained semiquantitatively along the following line of reasoning. If it is assumed that the photoionization efficiencies among the conformers are the same if the photon energy is higher than the threshold energies, then the height of the photoionization efficiency spectrum would be directly proportional to the concentration of the conformers. The cyclic conformer would have the lowest ionization threshold energy because its ionic state has the highest interaction energy. The height of the first step in the photoionization efficiency spectrum would be a measure of the concentration of the cyclic conformer. As one moves to higher photon energy, two conformers with internal hydrogen bonding begin to set in. As the photon energy becomes higher than 30 000 cm^{-1}, the noncyclic conformers without internal hydrogen bonding begin to be ionized. The concentration ratio between the three types of conformers is about 5:8:1 at 303 K. This is consistent with the theoretical results of adiabatic dissociation energies of these conformers, which state that one of the two noncyclic conformers with internal hydrogen bonding, K(tGg′), has the same adiabatic dissociation energy as the cyclic form while the other conformer, K(gGg′), is only about 1.9 kcal/mol higher than the cyclic form. The noncyclic conformers without internal hydrogen bonding have the smallest adiabatic dissocaition energies and thus the lowest concentrations.

4.3.2. K_2(en). The photoionization efficiency spectrum of K_2(en) is shown in the upper half of Figure 10 and its logarithmic plot is shown in the lower part. There are three general features of the spectrum: (a) well-defined conformation structures are not observed; (b) the ionization threshold region rises much slower than that of the spectrum of K(en); and (c) the Watanabe plot in the rising threshold region is not all that linear. It is recognized that for K(en) the photoionization strength comes from the valence electron of K, and for K_2(en) it comes from K_2. K_2(en) has three more vibrational degrees of freedom than K(en) in contributing

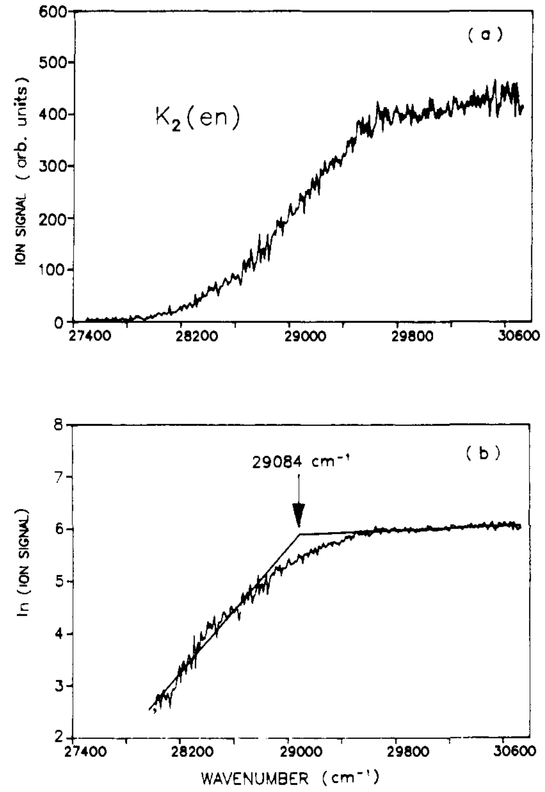

Figure 10. Photon-number-normalized photoionization efficiency spectrum (a) and the Watanabe plot of K_2(en) at 303 K (b).

to the photoionization spectrum, which would give the present spectrum a longer thermal ionization tail. As mentioned previously, the dissociative ionization process may compete with the direct ionization one. In order to elucidate this problem, the energy differences between K_2^+(en) and the dissociated system, K and K^+(en), were also calculated. The results show that, except for K_2^+(g′Gg′), all of the K_2^+(en) conformers are less stable than the K and K^+(g′Gg′) system. This indicates that all of the K_2^+(en) conformers, except for K_2^+(g′Gg′), generated by laser pulses would eventually dissociate into K and K^+(g′Gg′) adiabatically. On the basis of these energetic relations, the single rising step of the photoionization efficiency spectra of K_2(en) was assigned as the photoionization of the cyclic K_2(g′Gg′) conformer. The long thermal tail and the pronounced nonlinearity in the Watanabe plot are due to the three extra vibrational degrees of freedom of the second potassium atom. Because this potassium bonding is relatively weak, the thermal population is expected to be important for its vibrational motion. The photoionization threshold energy is determined to be 3.57 ± 0.05 eV with the Watanabe method. The uncertainty was estimated from the uncertainty of the linear regime in the Watanabe plot. This measured value is in reasonably good agreement with the theoretical vertical ionization energy of the cyclic conformer if one offsets the theoretical value with the difference between the experimental and theoretical ionization potentials of K_2.

4.4. Bond Dissociation Energies of K(en), K_2(en), K^+(en), and K_2^+(en). There are three commonly used measures of the bond strength of a molecule: equilibrium bond dissociation energy (D_e), bond dissociation energy (D_0), and enthalpy of bond dissociation ($\Delta H°_T$; T, absolute temperature). In the case that a molecular complex dissociates into an atomic species and a molecule, to a good approximation, these three quantities are related to each other through statistical mechanics by the following relations:

$$\Delta H°_T = D_e - {}^5\!/_2RT + \sum^{\text{prod}} \sum_i^n \frac{N}{2}\, h\nu_i - \sum^{\text{react}} \sum_i^m \frac{N}{2}\, h\nu_i + RT^2\Big[\sum^{\text{prod}} \sum_i^n (\partial \ln Q_{\nu_i}/\partial T) - \sum^{\text{react}} \sum_i^m (\partial \ln Q_{\nu i}/\partial T)\Big] \quad (4)$$

where N is Avogadro's number, R is the gas constant, and $Q_\nu = \sum_i^n[1 - \exp(-h\nu_i/kT)]^{-1}$, the vibrational partition function. D_0 and D_e are related by

$$D_0 = D_e + \sum^{\text{prod}} \sum_i^n \frac{N}{2} h\nu_i - \sum^{\text{react}} \sum_i^m \frac{N}{2} h\nu_i \quad (5)$$

In thermodynamic measurements, one usually obtained $\Delta H°_T$ over a certain range of temperature. In the experiments of photoionization, photodissociation, or spectroscopic measurement, the directly related energy quantity is D_0. However, for theoretical studies, the energy quantity obtained first is D_e. For the dissociation process of a comparatively weak bond, the temperature correction term in the enthalpy of dissociation is usually within 1 kcal/mol as far as the temperature range is on the order of room temperature.[32] As for the zero-point vibrational energy correction term, the magnitude is similar if the bonding strengths and bonding atoms of the complexes are similar to each other.

For the potassium–ethylenediamine systems, a full evaluation of the vibrational contribution to the enthalpy or entropy would require a complete potential surface of all of the low vibrational modes, which includes the conformational motion.[33] In the present photoionization study and in the reported experimental measurements of the enthalpy of the formation K^+(en), the cyclic conformer was always the main species involved. In other words, the contribution of the conformational change is not so important as long as the temperature is kept on the low side. For the present consideration, because of the similar interaction strengths between $K^+(CH_3NH_2)$ and K^+(en) and between $K(CH_3NH_2)$ and K(en), to a good approximation, the correction factors of the $K(CH_3NH_2)$ and $K^+(CH_3NH_2)$ complexes were used as reference systems for K(en) and K^+(en), respectively. With the help of the above energy relations and the theoretical harmonic vibrational frequencies of CH_3NH_2 and $K^+(CH_3NH_2)$, one finds that the enthalpy of dissociation of $K^+(CH_3NH_2)$ is higher than its bond dissociation energy by 0.5 kcal/mol at 298 K and lower by a value of 1.3 kcal/mol at 660 K. Its vibrational zero-point energy correction is −1.6 kcal/mol (relative to D_e). In the same way, the vibrational zero-point energy correction is calculated to be −1.3 kcal/mol for $K(CH_3NH_2)$. In the following discussion we shall use these values as estimations for the corresponding correction terms in the K(en) and K^+(en) systems. The enthalpy of dissociation of $K^+(CH_3NH_2)$ at room temperature was measured to be 19.1 kcal/mol.[34] By taking the correction of the heat capacities and the zero-point energy correction terms into account, the bond dissociation energy was recalculated to be 18.6 kcal/mol. The theoretical value is 16.7 kcal/mol at the level of MP2/6-31g*. The agreement is very good.

The enthalpy of the dissociation of K^+(en) has been measured to be 25.7 kcal/mol at 660 K.[35] The K^+(g′Gg′) conformer is the major species involved in this experiment. Compared with the theoretical equilibrium dissociation energy of 30.9 kcal/mol, and taking into account both the thermal energy correction (−1.3 kcal/mol) and zero-point vibrational energy correction (−1.6 kcal/mol), the agreement between theory and experiment is within 2.5 kcal/mol. Note that in the above theoretical calculation, we only consider the dissociation of the ionic complex into the most stable conformer of ethylenediamine. On the basis of this conformer, a slightly higher theoretical prediction is expected in this comparatively high temperature regime.

The equilibrium geometries of the ionic and neutral states of the cyclic conformer are similar to each other. One could well approximate the threshold ionization potential as the adiabatic ionization potential. Taking the experiment enthalpy of the dissociation of K^+(en) to be 25.7 kcal/mol at 660 K, the correction for the enthalpy of ionic complex dissociation to be −1.3 kcal/mol, the ionization potential of K to be 4.34 eV (100.1 kcal/mol), and

---

[32] Keesee, R. G.; Castleman, A. W., Jr. *J. Phys. Chem. Ref. Data* **1986**, *15*, 1011–1071.

[33] Nagy, P. I.; Dunn, W. J., III; Alagona, G.; Ghio, C. *J. Am. Chem. Soc.* **1991**, *113*, 6719–6729.

[34] Davidson, W. R.; Kebarle, P. *J. Am. Chem. Soc.* **1976**, *98*, 6133–6138.

[35] Davidson, W. R.; Kebarle, P. *Can. J. Chem.* **1976**, *54*, 2594–2599.

J. Am. Chem. Soc. **1992**, *114*, 9177–9181

the ionization potential of the cyclic conformer to be 3.34 eV (77.0 kcal/mol), one obtains an approximate bond dissociation energy with respect to conformer tGg′ of 3.9 kcal/mol for the K(g′Gg′) conformer. The theoretical equilibrium bond dissociation energy is 4.8 kcal/mol. If one takes the zero-point vibrational energy correction of −1.3 kcal/mol into account, the agreement is excellent.

In this study, the upper bound of the enthalpy of K_2(en) dissociation has been determined to be 10.4 kcal/mol at 300 K. This is consistent with the theoretical dissociation energy of 7.4 kcal/mol. Approximating the upper bound of the bond dissociation energy of K_2(en) to be 10,4 kcal/mol and taking the photoionization potentials of K_2 and K_2(en) to be 4.06 eV (93.6 kcal/mol) and 3.47 eV (82.3 kcal/mol), respectively, one obtains the upper bound of the bond dissociation energy K_2^+(en) as 21.3 kcal/mol. The theoretical equilibrium adiabatic bond dissociation energy of K_2^+(g′Gg′) is 22.3 kcal/mol. The consistency between these two values is good.

5. Conclusions

The following conclusions can be drawn from the results of the present photoionization and molecular orbital calculation studies of K(en) and K_2(en).

(a) The basic types of the conformers of K(en) can be generated in a flow reactor, and the photoionization efficiency spectrum can be resolved and interpreted. Only the most stable conformer of K_2(en) was detected by photoionization mass spectrometry at room temperature.

(b) For K(en), the nature of the bonding between the potassium atom and the two amino groups is essentially the same as that of $K{-}NH_3$ or $K{-}CH_3NH_2$, whether the potassium bond is in the bidentate (cyclic form) or monodentate form (noncyclic form). For K_2(en), the bonding energies are consistently larger than those of K(en). The charge polarization effect of K_2 by ethylenediamine contributes the additional stabilization for the dipotassium systems.

(c) The bond dissociation energies of K(en), K_2(en), K^+(en), and K_2^+(en) are internally consistent with each other through energy cycles, both theoretically and experimentally. For the ionization potentials of K(en) and K_2(en), the agreements between the theoretical results and the experimental values are also good.

Acknowledgment. This work is financially supported by the National Science Council, Republic of China.

Derivatization of the Fullerene Dications C_{60}^{2+} and C_{70}^{2+} by Ion–Molecule Reactions in the Gas Phase

Simon Petrie, Gholamreza Javahery, Jinru Wang, and Diethard K. Bohme*

Contribution from the Department of Chemistry and Centre for Research in Earth and Space Science, York University, North York, Ontario M3J 1P3, Canada. *Received April 23, 1992*

Abstract: Ion–molecule addition reactions which lead to the bonding of the fullerene dications C_{60}^{2+} and C_{70}^{2+} with various neutral molecules, most notably unsaturated hydrocarbons and amines, have been studied using a SIFT apparatus at a pressure of 0.40 ± 0.01 Torr and a temperature of 294 ± 2 K. The efficiency of adduct formation in these reactions shows a dependence upon the ionization energy, the size, and the degree of unsaturation of the molecules in question. A model is presented which relates the efficiency of adduct formation to these parameters.

Introduction

The recent discovery[1] and synthesis[2] of the fullerene series of carbon molecules has provoked a widespread and multifaceted investigation into the properties of these molecules. The ion–molecule reactivity of these species is one area of considerable interest. High-energy collision experiments, for example, have dealt with the competition between fragmentation and incorporation of small neutrals within the fullerene cage.[3-5] In the thermal energy regime, studies to date have focused both on bracketing the first three ionization energies[6-8] and the proton affinity of C_{60} and C_{70}[9] and on the occurrence of (exohedral) adduct formation in some reactions of atomic ions with C_{60}.[10]

The unique resilience of the fullerene cage and the multiplicity of charge states of fullerenes accessible to various experimental techniques makes them a fascinating field of study. We have recently begun an extensive study of the ion–molecule reactivity of fullerenes[11] and fullerene cations and dications[8,12,13] using the Selected-Ion Flow Tube (SIFT) technique. An area of special interest is the reactivity of the dications C_{60}^{2+} and C_{70}^{2+}. While several studies have been reported on the ion–molecule reactivity of atomic dications, notably the doubly-charged rare gas ions He^{2+}, Ne^{2+}, Ar^{2+}, Kr^{2+}, and Xe^{2+},[14] and while much effort has gone into characterising the second ionization energies of many molecules by techniques such as charge stripping,[15] double charge transfer,[16] electron impact[17] and photoionization,[18] very little

---

(1) Kroto, H. W.; Heath, J. R.; O'Brien, S. C.; Curl, R. F.; Smalley, R. E. *Nature* **1985**, *318*, 162.

(2) Krätschmer, W.; Lamb, L. D.; Fostiropoulos, K.; Huffmann, D. R. *Nature* **1990**, *347*, 354.

(3) (a) Weiske, T.; Bohme, D. K.; Hrusak, J.; Krätschmer, W.; Schwarz, H. *Angew. Chem., Intl. Ed. Engl.* **1991**, *30*, 884. (b) Weiske, T.; Hrusak, J.; Bohme, D. K.; Schwarz, H. *Chem. Phys. Lett.* **1991**, *186*, 459. (c) Weiske, T.; Hrusak, J.; Bohme, D. K.; Schwarz, H. *Helv. Chim. Acta* **1992**, *75*, 79. (d) Weiske, T.; Wong, T.; Krätschmer, W.; Terlouw, J. K.; Schwarz, H. *Angew. Chem., Intl. Ed. Engl.* **1992**, *31*, 183.

(4) Ross, M. M.; Callahan, J. H. *J. Phys. Chem.* **1991**, *95*, 5720.

(5) (a) Wan, Z.; Christian, J. F.; Anderson, S. L. *J. Chem. Phys.* **1992**, *96*, 3344. (b) Christian, J. F.; Wan, Z.; Anderson, S. L. In preparation.

(6) Zimmerman, J. A.; Eyler, J. R.; Bach, S. B. H.; McElvany, S. W. *J. Chem. Phys.* **1991**, *94*, 3556.

(7) (a) McElvany, S. W.; Ross, M. M.; Callahan, J. H. *Proc. Mat. Res. Soc. Symp.* **1991**, *206*, 697. (b) McElvany, S. W.; Bach, S. B. H. *Conf. Mass Spectrom. Allied Topics* **1991**, *39*, 422.

(8) Petrie, S.; Javahery, G.; Wang, J.; Bohme, D. K. *J. Phys. Chem.* **1992**, *96*, 6121.

(9) McElvany, S. W.; Callahan, J. H. *J. Phys. Chem.* **1991**, *95*, 6187.

(10) (a) Roth, L. S.; Huang, Y.; Schwedler, J. T.; Cassady, C. J.; Ben-Amotz, D.; Kahr, B.; Freiser, B. S. *J. Am. Chem. Soc.* **1991**, *113*, 6298. (b) Huang, Y.; Freiser, B. S. *J. Am. Chem. Soc.* **1991**, *113*, 8186. (c) Huang, Y.; Freiser, B. S. *J. Am. Chem. Soc.* **1991**, *113*, 9418.

(11) Javahery, G.; Petrie, S.; Wang, J.; Bohme, D. K. *Chem. Phys. Lett.* **1992**, *195*, 7.

(12) Petrie, S.; Javahery, G.; Wang, J.; Bohme, D. K. *J. Am. Chem. Soc.* **1992**, *114*, 6268.

(13) Bohme, D. K.; et al. In preparation.

(14) See, for example: (a) Smith, D.; Grief, D.; Adams, N. G. *Int. J. Mass Spectrom. Ion Phys.* **1979**, *30*, 271. (b) Viggiano, A. A.; Fehsenfeld, F. C.; Villinger, H.; Alge, E.; Lindinger, W. *Int. J. Mass Spectrom. Ion Phys.* **1981**, *39*, 1. (c) Störi, H.; Alge, E.; Villinger, H.; Egger, F.; Lindinger, W. *Int. J. Mass Spectrom. Ion Phys.* **1979**, *30*, 263. (d) Okuno, K.; Koizumi, T.; Kaneko, Y. *Phys. Rev. Lett.* **1978**, *40*, 1708. (e) Horning, S. R.; Kotiaho, T.; Dejarme, L. E.; Wood, J. M.; Cooks, R. G. *Int. J. Mass Spectrom. Ion Processes* **1991**, *110*, 1.

(15) Kemp, D. L.; Cooks, R. G. In *Collision Spectroscopy*; Cooks, R. G., Ed.; Elsevier: Amsterdam, 1978; p 257.

0002-7863/92/1514-9177$03.00/0